Modelling commercial vehicle handling and rolling stability

K Hussain*, **W Stein,** and **A J Day**
School of Engineering, Design, and Technology, University of Bradford, Bradford, UK

The manuscript was received on 3 September 2004 and was accepted after revision for publication on 28 April 2005.

DOI: 10.1243/146441905X48707

Abstract: This paper presents a multi-degrees-of-freedom non-linear multibody dynamic model of a three-axle heavy commercial vehicle tractor unit, comprising a subchassis, front and rear leaf spring suspensions, steering system, and ten wheels/tyres, with a semi-trailer comprising two axles and eight wheels/tyres. The investigation is mainly concerned with the rollover stability of the articulated vehicle. The models incorporate all sources of compliance, stiffness, and damping, all with non-linear characteristics, and are constructed and simulated using automatic dynamic analysis of mechanical systems formulation. A constant radius turn test and a single lane change test (according to the ISO Standard) are simulated. The constant radius turn test shows the understeer behaviour of the vehicle, and the single lane change manoeuvre was conducted to show the transient behaviour of the vehicle. Non-stable roll and yaw behaviour of the vehicle is predicted at test speeds >90 km/h. Rollover stability of the vehicle is also investigated using a constant radius turn test with increasing speed.

The articulated laden vehicle model predicted increased understeer behaviour, due to higher load acting on the wheels of the middle and rear axles of the tractor and the influence of the semi-trailer, as shown by the reduced yaw rate and the steering angle variation during the constant radius turn. The rollover test predicted a critical lateral acceleration value where complete rollover occurs. Unstable behaviour of the articulated vehicle is also predicted in the single lane change manoeuvre.

Keywords: commercial vehicle, dynamics, articulated, multibody dynamics, handling, stability, rollover

1 INTRODUCTION

Heavy goods vehicles (HGVs) are the main transportation system of goods via roads worldwide. Several studies have reported that a significant proportion of serious road accidents involve lack of HGV stability. The US National Highway Traffic Safety Administration reported that, in 2000, $\sim$13 per cent of all accidents involved rollover of commercial vehicles [**1**]. Because of this high rate of reported accidents, safety issues with these vehicles have become increasingly important and legislation has been introduced for manufacturers and drivers.

In recent years, a driver licence handbook for commercial vehicles shows some important safety factors that apply specifically to articulated vehicles [**2**]. Characteristics such as rollover risk, which could be caused by carrying high loads, the influence of sudden steering, and jack-knifing are all explained in detail in the handbook.

During the past two decades, the study of vehicle dynamics has generated great advances. Gillespie [**3**], Dixon [**4**], Ellis [**5**], and Pacejka [**6**] presented the fundamentals of vehicle dynamics including the analysis of two axled vehicles. The suspension characteristics and the basics of vehicle handling for steady state and transient manoeuvres for simplified vehicle models have also been analysed. The use of multibody dynamic simulation of road vehicles (cars) has been recently demonstrated by Rahnejat [**7**], Hegazy [**8**, **9**] and Blundell and Harty [**10**].

**Corresponding author: School of Engineering, Design, and Technology, University of Bradford, Bradford, West Yorkshire BD7 1DP, UK.*

Genta [**11**] showed the behaviour of a two-axle truck and the influence of a semi-trailer on such a vehicle. The equations of motion for rigid and articulated vehicles were presented and their performance was assessed.

Lin *et al.* [**12**] performed static and dynamic tests on an articulated vehicle to validate a non-linear vehicle simulation. A simple linear model was developed to investigate three different roll strategies: roll angle, lateral load transfer, and lateral acceleration feedback. Sampson [**13**] described the use of an active roll control system, consisting of active anti-roll bars to improve the roll stability of rigid and articulated heavy vehicles.

Even though most studies have concentrated on rigid vehicles, Aurell [**14**] showed the importance of taking chassis flexibility into account by the development of a warp model. The influence of the torsional stiffness of the chassis on the yaw stability of the vehicle was also investigated by Aurell.

The main aim of this paper is to investigate, via computer-based multibody dynamic simulation, the handling and roll stability behaviour of commercial vehicles and to establish the critical vehicle speeds and steering angles at which roll occurs. Constructing a realistic full vehicle model was an essential part of investigating and testing the roll stability characteristics of these vehicles, and this comprised a tractor model with a non-linear truck tyre model, a steering model, and a leaf spring suspension system model. A semi-trailer model was also constructed and added to the tractor model to investigate the response of the combined tractor–trailer system. All simulations used the automatic dynamic analysis of mechanical systems (ADAMS) software [**15**] and the loading conditions were based on a standard test procedure for heavy commercial vehicles.

2 THE VEHICLE MODEL: TRACTOR

The tractor model was based on design data for a ten-wheel three-axle commercial vehicle designed and manufactured by the manufacturing company. This particular vehicle is commercially available throughout the world. The suspension and the steering systems are modelled and explained, and the vehicle data are presented.

2.1 Tractor vehicle model parts

The various parts of the tractor model were developed and shaped as closely as possible to the actual vehicle, as shown in Fig. 1, with the chassis structure of the vehicle modelled using rigid parts. A cab was mounted on the front of the chassis, and at the rear, a fifth wheel was created to attach the semi-trailer. From the axle masses, geometry, and material properties, the moments of inertia were determined by the ADAMS software. On each side of the front axle the wheel carriers, including the steering knuckle and the steering arm, were created.

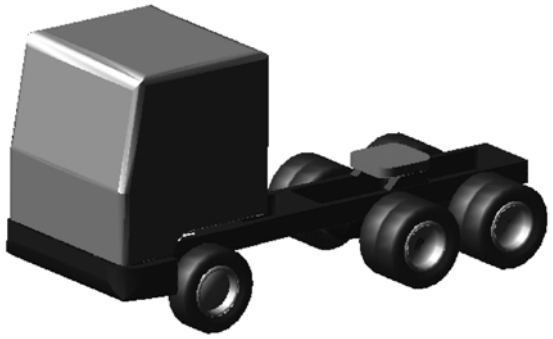

Fig. 1 Ten-wheel tractor model

2.2 Leaf spring suspension system

The vehicle suspension was based on rigid axles and leaf springs. A schematic diagram of a leaf spring is shown in Fig. 2. Forces are applied to the chassis at the front spring eye and the rear shackle attachment point on the chassis [**3**].

2.2.1 Tractor vehicle front suspension system

The front suspension of the tractor vehicle was a rigid axle mounted on two leaf springs (Fig. 2) and the ADAMS model was constructed as shown in Fig. 3(a). The leaf spring model was built using nine discrete beam elements, from which the ADAMS software computes, using the geometry and the material characteristics, the deflection of the elements due to the load. The height of the spring was calculated based on the simple beam theory. The various suspension data for each side of the front axle are given in Table 1, taken directly from the manufacturer's data sheet.

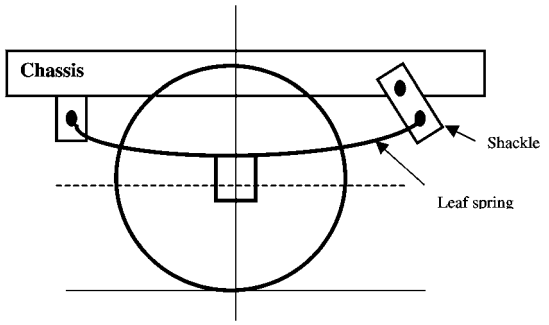

Fig. 2 Rigid axle leaf spring suspension

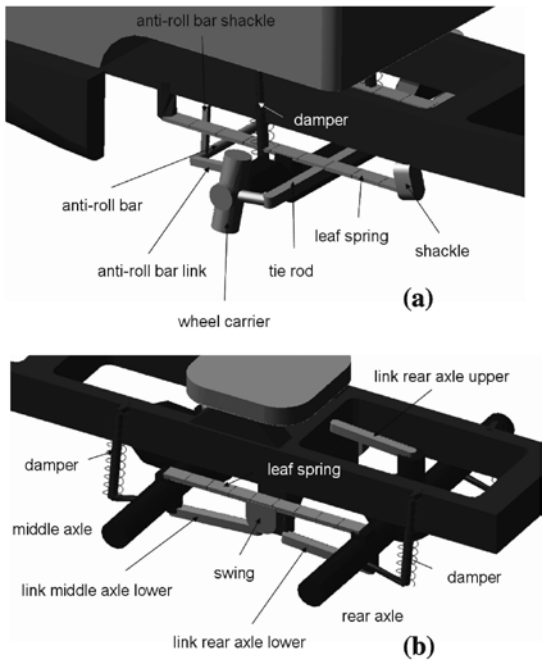

Fig. 3 (a) Front suspension and anti-roll device and (b) rear suspension

The front spring eye, at the front end of the leaf spring, was modelled as being attached to the chassis via a revolute joint lateral to the vehicle longitudinal axis. The front axle was connected to the leaf spring via a fixed joint at the mid-point of the leaf spring. The rear end of the leaf spring was fixed to the shackle also via a revolute joint, while the shackle was connected to the chassis in the same manner. Both joints were parallel to the front revolute joint. This system was tested via a separate virtual test rig to ensure the correct spring stiffness and position of the joints. The height of the spring was adjusted, as shown in Table 1, to achieve the correct stiffness. To avoid large deflection of the spring due to the sprung weight, an additional spring was used to apply a preload. The preload spring was placed between the front axle and the chassis at the centre of the axle and its stiffness is given in Table 1. Two dampers were added between the front axle and the chassis on each side of the vehicle.

Table 1 Front, middle, and rear suspension data

	Front	Middle	Rear
Spring stiffness (N/mm)	189.33	1084	1084
Spring width (mm)	90	90	90
Young's modulus (N/mm^2)	20.7×10^4	20.7×10^4	20.7×10^4
Spring length (mm)	1500	1300	1300
Spring height (calculated) (mm)	20.47	31.73	31.73
Spring height (adjusted) (mm)	20.70	31.80	31.80
Damping coefficient (Ns/m)	7870	35 000	26 000
Preload (entire axle) (N)	37 312	7950	7950

2.2.2 *Tractor vehicle rear suspension system*

In the rear suspension system of the tractor vehicle, there were two axles, defined as the middle axle and the rear axle (Fig. 3(b)). A leaf spring on each side of the chassis was fixed in the middle to a pivoted beam connected to the chassis via a central bearing. The springs could slide at each end on the axles in the longitudinal direction, but were fixed in the lateral direction. Hence, they were able to transmit lateral forces between the axle and the chassis.

Each axle had three links (two lower and one upper, as shown in Fig. 3(b)) to connect it with the subframe. This arrangement prevented the axle from twisting and carried the longitudinal forces between the axle and the chassis. The upper link of the middle axle was located 78 mm to the left side of the vehicle, measured to the vehicle centre line, and was attached 65 mm in front of the mid-point of the two axles. The upper link of the rear axle had a similar offset to the right side of the vehicle and was attached to the chassis, 135 mm behind the mid-point of the axles. The arrangement of the lower links was symmetrical to the right and the left sides and also to the middle and the rear axles. In the normal ride position, the links were inclined by 4° downwards towards the axles.

The lower links were connected to the chassis using a universal joint. For the attachment to the axles, a spherical joint was used, thus the axle was fixed in the longitudinal direction and its rotation was constrained. A dummy part connected the axle and the leaf spring with a slide joint between the axle and the dummy part. This joint allowed motion in the longitudinal direction and fixed all other directions and orientations. A revolute joint was added between the dummy part and the leaf spring in the lateral direction to allow a rotational motion between them, and a similar arrangement was made at each attachment point between the axle and the leaf spring. In this way, the lateral and the vertical degrees-of-freedom of the axles were also restrained. The centre of the spring was connected to the 'swing', see Fig. 3(b), via a fixed joint, and the swing was attached to the chassis with a revolute joint in the lateral direction. Thus, vertical motion of the rear and middle axles was possible without bending of the leaf spring. Such a vertical motion was controlled by a damper mounted between the axle and the chassis on each side of

the axle, as shown in Fig. 3(b). Data for the axles are given in Table 1.

2.3 Anti-roll device

To avoid large roll angles due to lateral acceleration and the high centre of gravity (CG) position, an anti-roll bar in the form of a U-shaped spring rod with a circular cross-sectional area was fitted to the actual vehicle at the front axle. This was modelled using beam elements. Both ends were fixed to the axle, while the central part was attached to each side to the chassis via a shackle, as shown in Fig. 3(a). The central part of the anti-roll bar, across the longitudinal vehicle centre line, thus had mainly torsion loading, whereas the end parts carried bending load. The central part was modelled using a discrete flexible bar with five elements and both end parts were constructed from rigid links between the front axle and the flexible bar. The links were connected to the front axle via a spherical joint and to the flexible bar by a fixed joint. The shackle was attached to the anti-roll bar using a revolute joint and the connection to the chassis was via a spherical joint.

2.4 Steering system

The steering axis inclination, camber, and caster values for the vehicle are shown in Table 2. The toe-in angle was set to zero. The Ackermann steering geometry data were not available from the manufacturer, so it was set as shown in Fig. 4; lines were drawn through the steering axis pivot point on each side of the vehicle to pass through the vehicle centreline at point P.

For Ackermann conditions the tie rod end position was at the intersection between these lines and the tie rod. The tie rod was set at 0.215 m behind the steering axis pivot point, and, by using the rule of proportion the position of the tie rod end was calculated as shown in Table 2. The tie rod was modelled using a link element, connected to the steering arms by a universal joint at one end and a spherical joint at the other.

Table 2 Steering data for the ten-wheel tractor model

Steering geometry	Value
Camber	0°
Caster	6°
Steering axis inclination	7°
Toe-in	0°
Centre position steering axis left	(0.0, −0.928, 0.524) m
Tie rod joint position left	(0.215, −0.905, 0.524) m

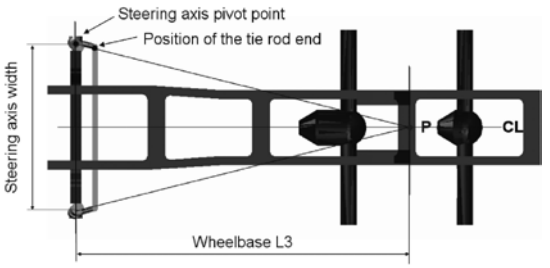

Fig. 4 Adjustment of Ackermann steering geometry

The wheel carriers were connected to the front axle by revolute joints, angled according to the king pin inclination and caster, as shown in Fig. 3.

2.5 Tyre model

The handling performance and directional response of a vehicle are greatly influenced by the forces and the moments generated by the tyres [**10**]. Accurate tyre representation is an important part of the simulation process. In this work, a tyre model was chosen based on the Magic Formula [**16**]. The tyre model used in this analysis was the standard tyre module within the ADAMS shared library [**15**] for a tyre with dimension 315/12.0R22.5, which is similar to those fitted on this vehicle.

The front wheels were connected to the front axle wheel carriers using revolute joints. The middle and the rear axle wheels were connected directly to the middle and the rear axles also using revolute joints.

3 SEMI-TRAILER MODEL

A two axle semi-trailer model was added to the tractor model, as shown in Fig. 5. All parts of the trailer were modelled as rigid parts, except the leaf springs which were built using discrete flexible links as for the rear suspension of the tractor model.

A damping coefficient of 35 000 Ns/m per damper and a preload for the entire semi-trailer of 71 230 N were used for the articulated vehicle model. Other data for the trailer are shown in Table 3; these were

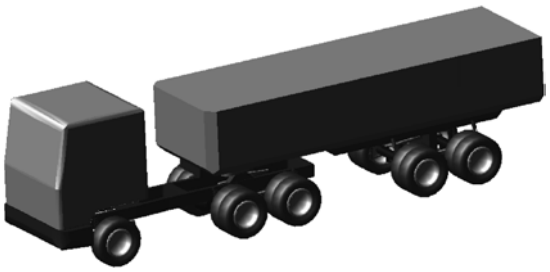

Fig. 5 Articulated tractor–trailer vehicle

Table 3 Articulated vehicle data

	Value
Trailer data	
Wheelbase (fifth wheel to trailer front axle)	4.0 m
Axle separation	1.3 m
Distance (fifth wheel to trailer CG)	2.5 m
Distance (fifth wheel to rear tractor axle)	0.26 m
CG height of the trailer	2.0 m
I_{xx}	30 000 kgm^2
I_{yy}	279 000 kgm^2
I_{zz}	285 000 kgm^2
Total mass	30 900 kg
Tractor geometry data	
Front track width	2.040 m
Rear and middle track width	1.85 m
Distance (front axle to CG)	1.83 m
Distance (CG to middle tractor axle)	1.22 m
Distance (CG to rear tractor axle)	2.52 m
CG height of the tractor	0.864 m
Tractor modified damping and preload data	
Tractor front axle damping coefficient	15 000 Ns/m
Tractor rear and middle damping coefficient	35 000 Ns/m
Preload entire tractor front axle	47 200 N
Preload entire tractor middle and rear axle	73 482 N

obtained from the vehicle manufacturer. The longitudinal CG position was chosen to achieve a similar static weight distribution for the tractor middle and rear axles and the trailer axles. The semi-trailer load acted at the fifth wheel position, so the preload and the damping values of the tractor were modified accordingly.

The trailer was joined to the tractor using a revolute joint in vertical direction. The chassis of the tractor and the trailer were both rigid, so to allow a relative angular roll motion between both parts of the vehicle a revolute joint was modelled in the horizontal direction at the fifth wheel position attached to a dummy part, with a torsional spring damper combination to simulate the torsional stiffness of the trailer chassis.

4 SIMULATION RESULTS AND DISCUSSION

Two types of test were implemented on the tractor model and the tractor–trailer model; a single lane change test and a rollover test. The results of the simulation of these tests are presented and discussed.

4.1 Single lane change

The single lane change manoeuvre test was carried out to assess the transient behaviour of the vehicle. The test was carried out under constant speed while negotiating a lane change, along a test path similar to that used by Da Cunha [**17**] as shown in Fig. 6(a). In this test configuration, the vehicle is driven in a straight line for 40 m; it then negotiates a turn for further 40 m and finally finishes with a 40 m straight line drive. The vehicle thus negotiates a lane change of 3.65 m offset within a distance of 40 m at three vehicle speeds: 90, 70, and 50 km/h. The parameters investigated included the tyre forces, particularly on the inside wheels as the vertical force diminishes with increasing lateral acceleration, and the vertical excursion of the front and rear roll centres as any large displacement of these can affect vehicle stability.

The steering function used for the single lane change manoeuvre was a sinusoid, and was achieved by using the 'step function' command in ADAMS.

Figures 6(b) and (c) show the animated output for the transient manoeuvre during a simulation of 10 and 15 s for both the unladen and the laden conditions, respectively. After an initial static equilibrium analysis was carried out to ensure vehicle placement at the kerb height, 1000 time steps of simulation were undertaken.

Figure 7(a) shows the lateral acceleration of the vehicle during the manoeuvre for the three test speeds. The lateral acceleration follows the steering command and increases for higher speeds. In a turn to the left, a negative lateral acceleration is predicted, which indicates a force towards the right side of the vehicle. When the steering angle changes the direction, the lateral acceleration also changes the direction. Maximum lateral predicted acceleration amplitudes of 0.39, 0.27, and 0.15 g were predicted at vehicle speeds of 90, 70, and 50 km/h, respectively.

Figure 7(b) shows the predicted lateral acceleration of the tractor. It is noticeable that higher lateral acceleration occurs during the second part of the manoeuvre, the right turn. A maximum lateral acceleration of 0.25 g was predicted for the highest speed (70 km/h) and the right turn. During the initial left turn, a predicted lateral acceleration value of 0.23 g was reached.

Figures 8(a) and (b) show the roll angle during the lane change maneouvre. The maximum roll angle predicted at 90 km/h speed was $\sim 0.62^\circ$, for 70 km/h a value of 0.43° was reached, and for the lowest speed of 50 km/h the maximum roll angle was 0.26°. The reason for these low roll values is that the height of CG was low when compared with the track width of the vehicle. In addition, the anti-roll device at the front axle prevents excessive roll, supported by high spring stiffnesses of the rear axle leaf springs.

Figure 8(b) shows the roll angle of the tractor for various test speeds. As expected, the roll angle for the right turn is also higher than that for the initial left turn, as higher lateral acceleration occurs during the second part of the manoeuvre. However,

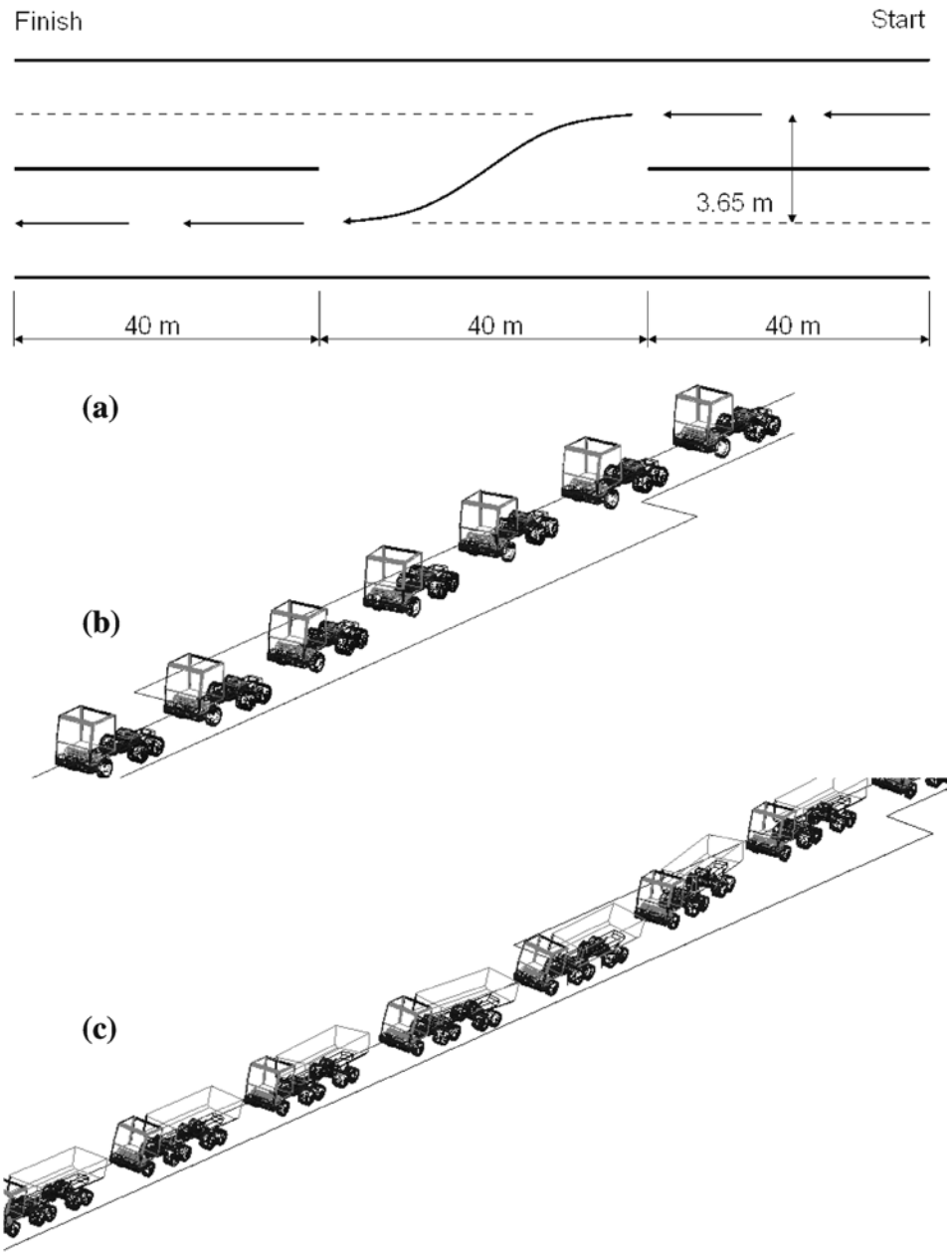

Fig. 6 (a) Lane change track and section designation manoeuvre test; (b) tractor lane change manoeuvre for 5 s of simulation; and (c) tractor–trailer lane change manoeuvre for 5 s of simulation

the influence of the coupling between the tractor and the trailer leads also to roll angle oscillation of the tractor, although the lateral acceleration shows small oscillation. This leads to predicted maximum roll angles of 4.9° for a test speed of 70 km/h, 3.5° for 50 km/h, and 1.1° for 30 km/h.

Figure 8(c) shows the roll angle of the trailer. The predicted trailer roll angles exceed those of the tractor. The predicted maximum of 9° was reached during the right turn at a speed of 70 km/h, in comparison, 6° for 50 km/h and 2° for 30 km/h. The predicted instability of the investigated tractor-trailer vehicle is shown here by the extensive trailer oscillation, which was evident from the lateral acceleration and roll behaviour.

4.2 Constant radius test

The constant radius turn manoeuvre which was simulated was similar to the SAE standard constant radius turn for heavy vehicles [**18**]; the vehicle was driven around a circular path of 75.0 m constant radius. A maximum test speed of 15 m/s was set to avoid rollover. An initial speed of 2.5 m/s was

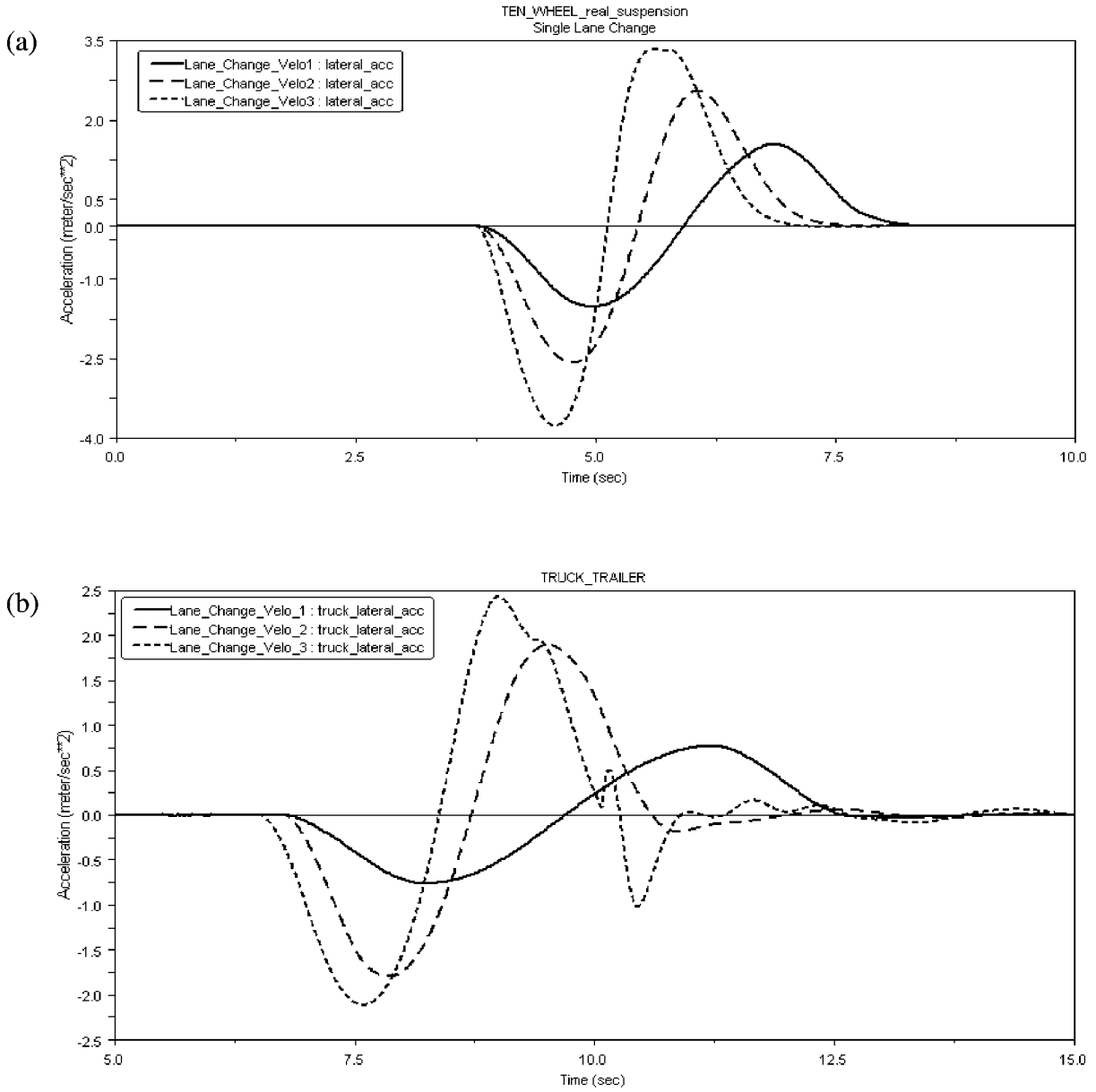

Fig. 7 (a) Lateral acceleration of the tractor model and (b) lateral acceleration of the tractor–trailer model

selected, which was then increased at a rate of 2.5 m/s until the maximum test speed was reached.

Figure 9(a) shows the predicted steering angle for various longitudinal speeds. A higher steering angle is observed at higher speeds, which indicates a tendency to understeer.

Figure 9(b) shows the lateral acceleration of the truck for various test speeds. A peak acceleration of 3.3 m/s^2 is reached at 15 m/s, which is close to the critical lateral acceleration of 3.7 m/s^2 when rollover occurs. A steady state lateral acceleration of 0.1 m/s^2, for 2.5 m/s test speed, was attained after 3 s, while a steady state lateral acceleration of 3 m/s^2 occurred after 6 s for the 15 m/s speed. The trailer attained similar steady state values.

Figure 9(c) shows the yaw rate for the tractor. The transient part shows a slight oscillation with increasing amplitudes for higher speeds. Similar to the lateral acceleration, the changeover to the steady state yaw rate takes longer for higher speeds. The steady state yaw rates for the six tests speeds from 2.5 to 15 m/s are about 2°/s, 3°/s, 6°/s, 7.5°/s, 9°/s, and 11°/s, respectively.

Figure 9(d) shows the yaw rate of the trailer. Although the steady state values are similar to the values of the tractor, the transient part shows

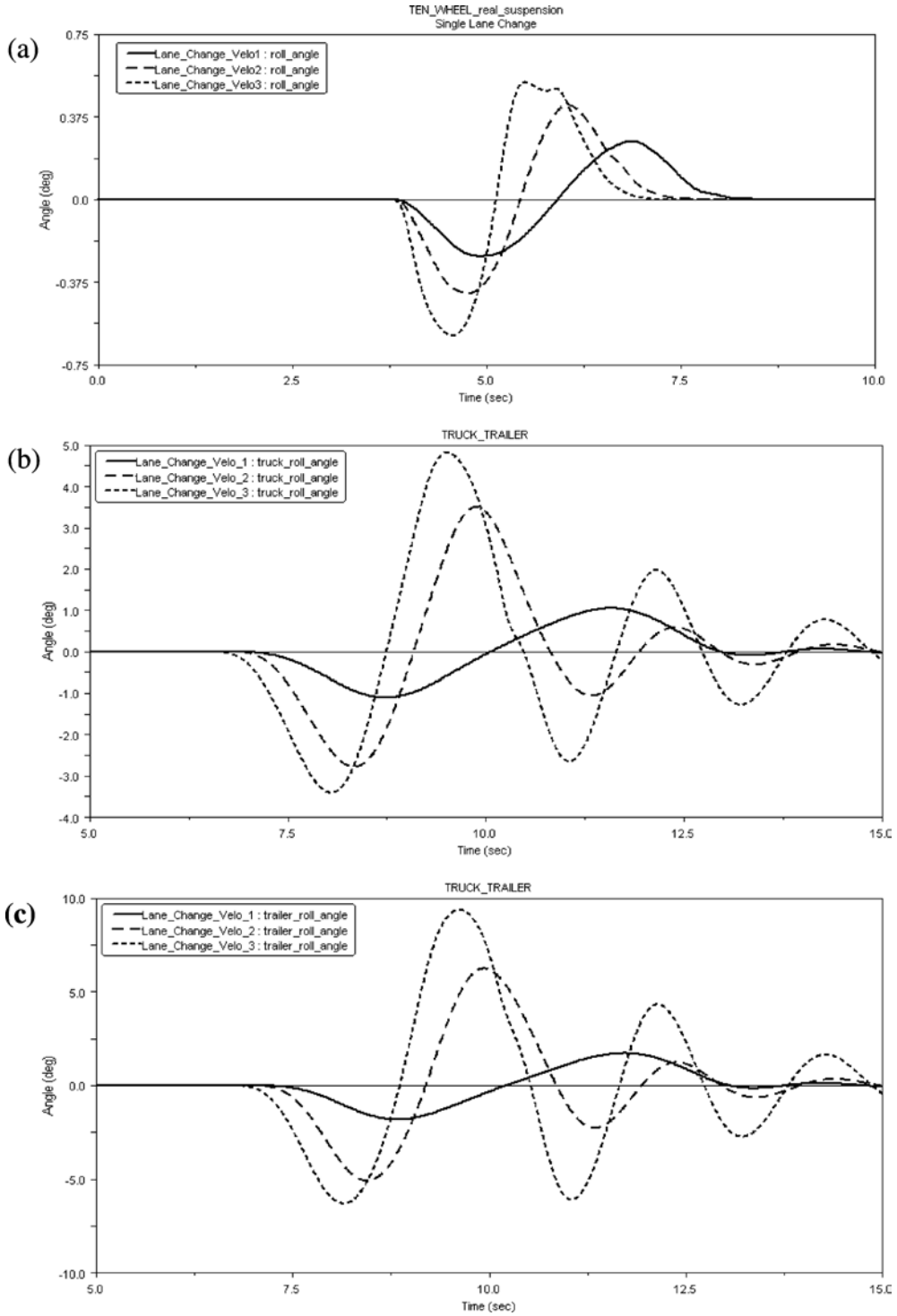

Fig. 8 (a) Tractor roll angle during single lane change manoeuvre and (b) tractor–trailer roll angle during single lane change manoeuvre (tractor section)

significant differences. The trailer shows higher amplitude oscillations in yaw rate at higher speeds.

4.3 Rollover test

Rollover (also called 'toppling') occurs when the inside wheels of a vehicle lift-off from the ground. It is one of the major problems associated with heavy commercial vehicles, particularly semi-trailer combinations, where in the majority of cases the rollover is initiated from the trailer [**19**]. The primary rollover factors are the CG, position of load, and effective track. Other secondary factors such as road camber, fifth wheel coupling, roll stiffness of

the suspension, torsional stiffness of the chassis, tyre pressures, and load shift also have an effect [**19**].

Vehicle roll induces suspension compression on the outer wheel and extension on the inner wheels. Suspension geometry design determines the magnitude of changes in steer angle during roll. Hence, some steering changes occur automatically as the vehicle rolls [**20**].

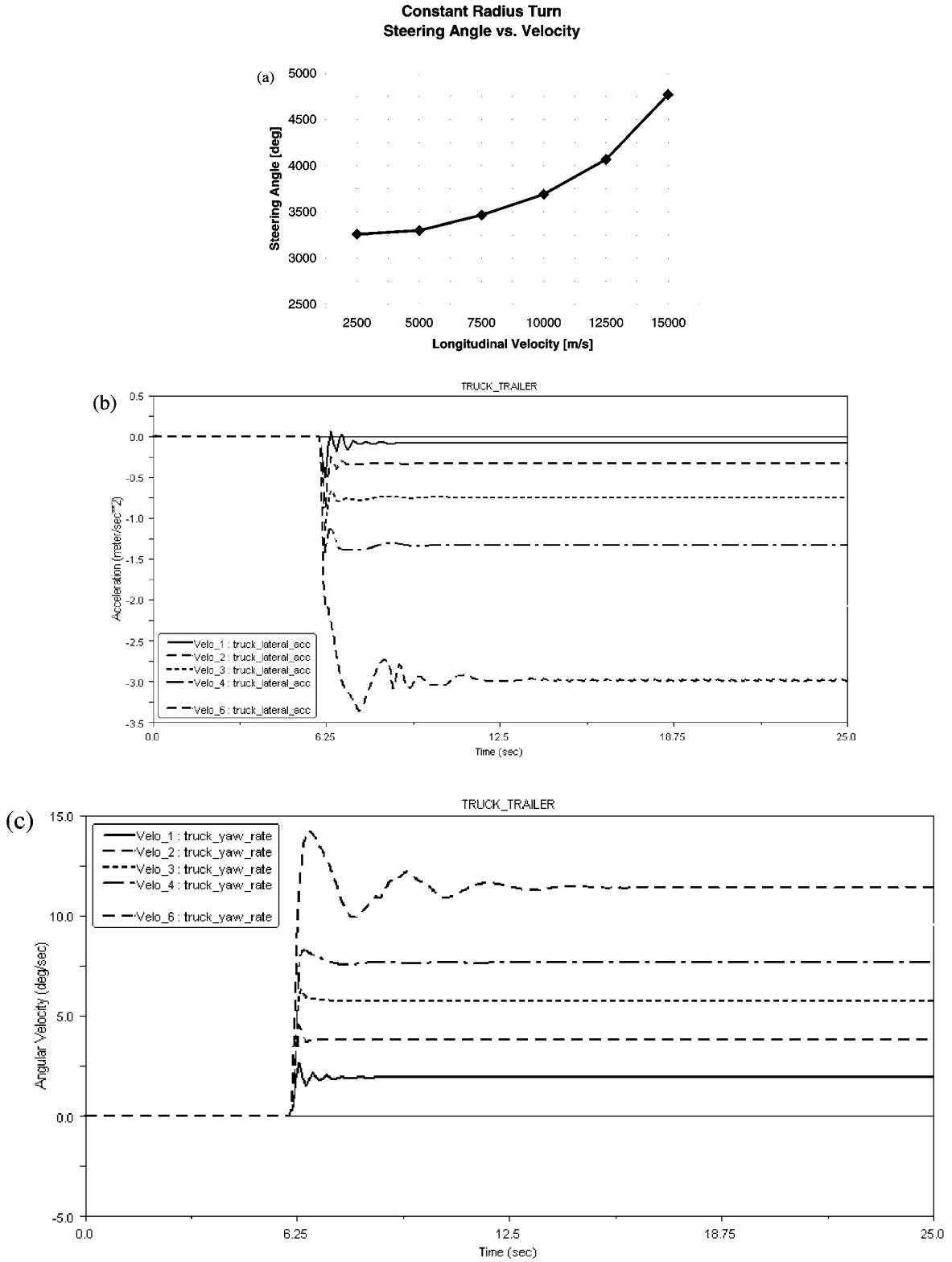

Fig. 9 (a) Steering angle versus longitudinal speed, constant radius turn; (b) tractor lateral acceleration; (c) tractor yaw rate; and (d) trailer yaw rate

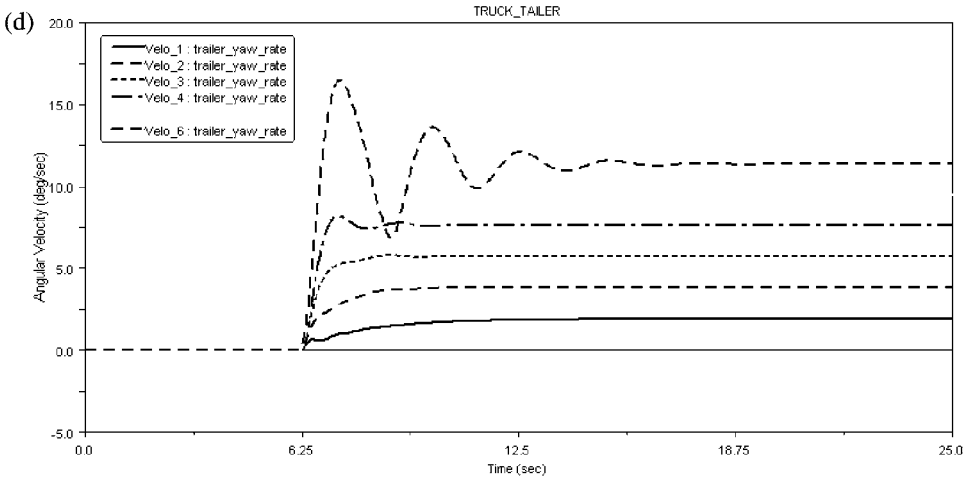

Fig. 9 Continued

The rollover test shows the predicted rollover instability of the vehicle. This was characterized by the lift of one or more vehicle wheels when the vertical force acting between tyre and ground reaches zero. A delay of 3 s at the beginning of the simulation was used to eliminate the effect of initial suspension oscillation, and a constant value of 4° steering angle was maintained to simulate left hand cornering. Figure 10 shows the transverse weight transfer for the front tyres (higher values) and the outer tyres of the rear axle (lower values). The increasing values represent the right side tyres and the decreasing values represent the left side. The left outer tyre of the rear axle has a final vertical force of 1900 N, which is the lowest value of all the tyres, therefore, no lift-off takes place, and hence, there would be no rollover predicted for this tractor in this manoeuvre.

For the tractor–trailer model, owing to the high CG position of the trailer, a rollover occurs after ∼63 s of the simulation time, for a steering angle of 4°. Figure 11 shows the articulated vehicle during the last stage of the rollover test when rollover occurs.

Figure 12(a) shows the increase of lateral acceleration until rollover occurs. The lateral acceleration increases uniformly to a value of 0.38 g for both tractor and trailer. A sudden change is predicted after 61 s, which indicates the beginning of a rollover of the tractor and the semi-trailer as the measured lateral acceleration rises sharply for both. The predicted lateral acceleration of 0.382 g is the limiting critical value for rollover.

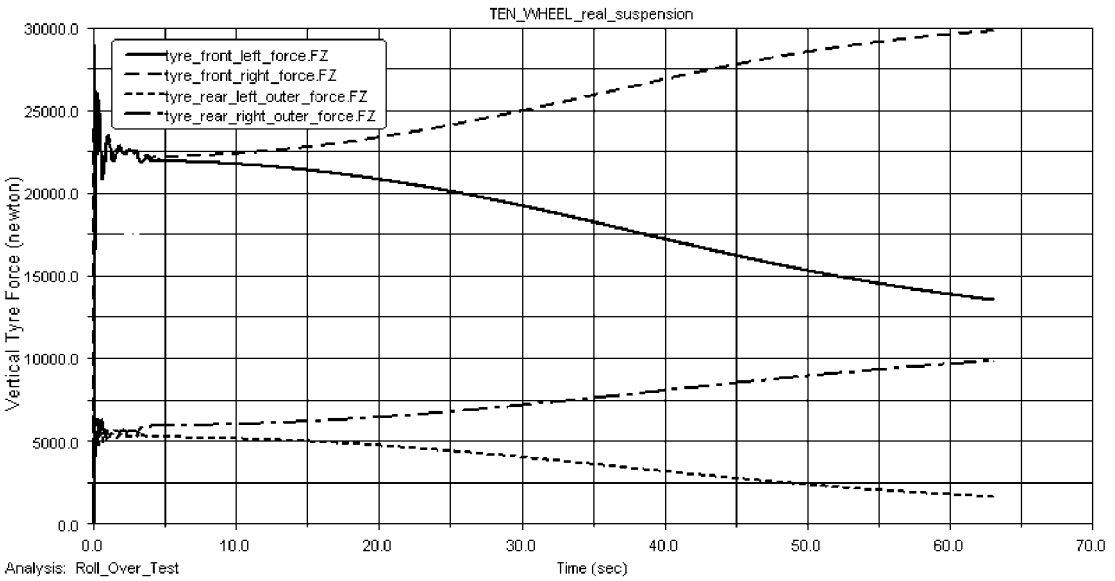

Fig. 10 Transverse weight transfer

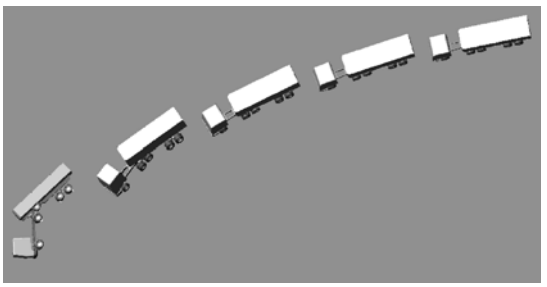

Fig. 11 Simulation of leading to rollover

However, a simple moment balance calculation for the limiting toppling of the trailer alone shows a critical lateral acceleration of 0.25 g. This indicated that the existence of the suspension and the interaction of the trailer with the tractor increase the limiting toppling lateral acceleration of the vehicle.

Figure 12(b) represents the weight distribution of the tractor front axle during the rollover cornering manoeuvre. Though the vertical force acting between the tyre and the ground increases on the right side (the vehicle follows left hand cornering), the left tyre vertical force is predicted to reach zero after 61 s. The final sharp decrease of the right tyre vertical force to zero shows the toppling of the vehicle. The onset of rollover for the trailer front axle is predicted to occur at a lateral acceleration of 0.378 g m/s^2. This value is lower compared with the limiting value of the entire vehicle, as rollover for the trailer occurs first, then the tractor follows.

Figure 12(c) shows the transverse weight transfer on the tractor rear axle. The middle axle was not investigated as its weight was lower than that of the rear axle. Similar to the front axle the right side force increases and the left side force decreases slightly until the front axle lifts off.

Figure 12(d) shows the tyre normal load distribution of the trailer rear axle, which is similar to that of the trailer front axle. The trailer right outer tyre vertical force increases until toppling of the vehicle takes place. The lift-off of the trailer is predicted to occur much earlier, after 50 s with a lateral acceleration of 0.323 g. Hence, the onset of rollover occurs first on the trailer, as mentioned earlier.

The predictions made using this multi-body dynamic model have not been experimentally verified because of the difficult and dangerous nature of such test work. There is also no published data relating to rollover performance of a specific commercial, articulated vehicle available in the literature. One reason for the research project was to establish whether multi-body dynamic simulation could predict, with some degree of accuracy, the rollover behaviour of articulated vehicles. However, despite the absence of direct validation, the results tend to agree with expert knowledge and understanding [**15**] in terms of the trends predicted.

For example, the rollover test simulation has shown the influence of the high CG position of the trailer. A moderate lateral acceleration of ∼0.38 g leads to a critical driving condition, and such conditions are all too easily experienced in everyday driving. Any torsional weakness of the trailer chassis could make the behaviour worse, as predicted here. A lower CG, achieved by design modification, will reduce the tendency for rollover. Other design modifications to the suspension, e.g. stiffer chassis, progressive suspension spring stiffness instead of a linear stiffness, and an anti-roll bar on the trailer

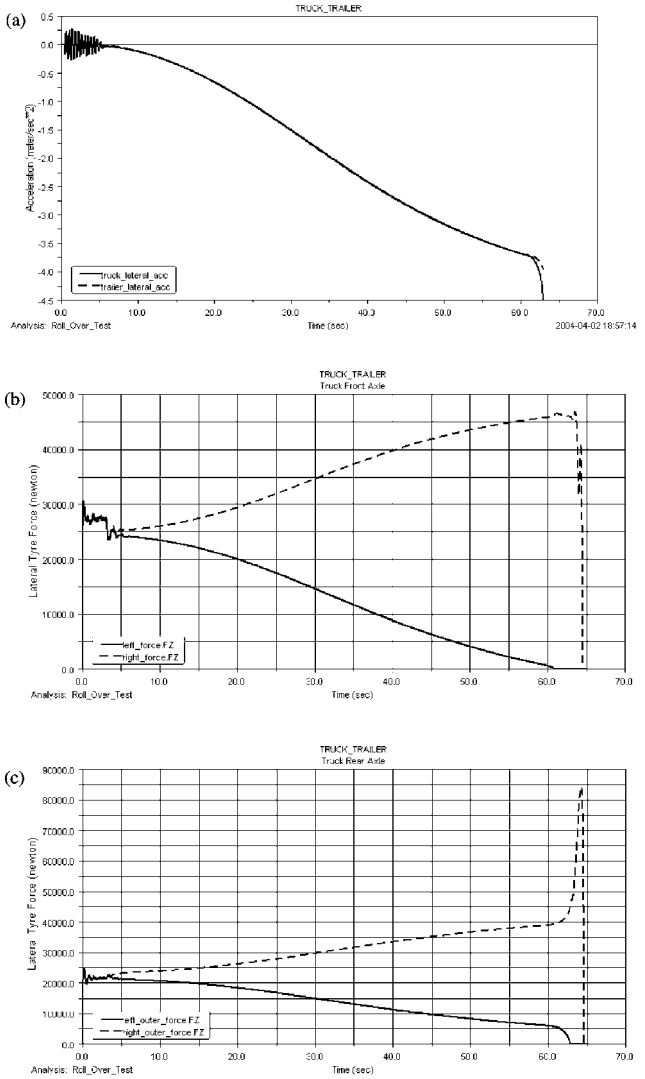

Fig. 12 (a) Lateral acceleration, rollover test; (b) transverse weight transfer, tractor front axle, rollover test; (c) transverse weight transfer, tractor rear axle, rollover test; and (d) transverse weight transfer, trailer rear axle, rollover test

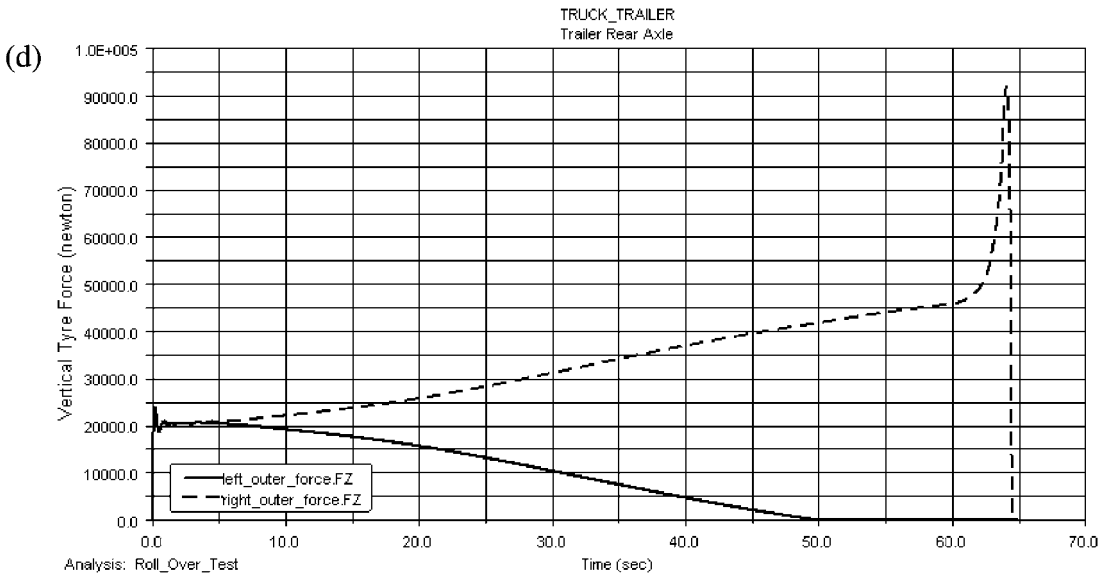

Fig. 12 Continued

axle could improve the rollover resistance of the articulated vehicle. All these could be investigated using the modelling approach presented here. The rollover resistance of the articulated vehicle could also be improved by (a) limiting roll steer effects and (b) limiting lateral displacement of the CG due to body roll. The most stable condition to reduce the possibility of rollover is for the CG to be over the rear wheels of the trailer with no load on the king pin [**19**]. However, such a load distribution may improve roll stability but can have an adverse affect on the tractor during braking, as the possibility of jack-knife increases dramatically [**19**]. Such a condition could be analysed and explained in detail using this modelling approach.

5 CONCLUSIONS

This paper has demonstrated the use of multibody dynamics in the predictive understanding of commercial heavy vehicle handling and rollover stability. A non-linear ten-wheel tractor/eight-wheel trailer virtual model, using geometric data obtained from a commercial vehicle manufacturer, has been presented. The model constructed includes leaf spring suspension systems, an anti-roll device, steering model, and a non-linear tyre model. Precise and detailed modelling of the subcomponents of the chassis system, in particular, the suspension links and spring contacts, has been shown to be necessary to achieve acceptable results. Such details have not been presented previously in published work.

The model was loaded with a transient single lane change manoeuvre similar to commercial vehicle handling standard tests specified in ISO 3888. The vehicle was also subjected to a rollover test to determine the wheel lift-off conditions; a wheel lift-off does not necessarily lead to rollover but describes a critical driving situation. The simulation of a single lane change has shown the transient behaviour of the vehicle in response to a sinusoidal steering input and vehicle stability of up to a maximum test speed of 90 km/h was predicted.

The simulation of the articulated vehicle model containing a three-axle tractor and a two-axle semi-trailer predicted the interaction and the cornering behaviour of the vehicle. The roll-over test for the articulated vehicle has shown that a critical lateral acceleration of 0.38 g would cause a rollover of the entire vehicle. It has also been shown that the understeer of the vehicle increased due to higher load and the influence of the trailer. The predicted tractor–trailer lateral acceleration was higher than that limited by toppling of the trailer alone. The single lane change simulation for the articulated vehicle predicted a loss of stability at 70 km/h.

Finally, it can be concluded that dynamic modelling and analysis of commercial vehicles can help designers to improve vehicle stability and, hence, increase the safety aspects of these vehicles to reduce road accidents. It is possible to assess the handling behaviour of a realistic commercial vehicle using virtual prototype in a multi-body dynamic system environment, as shown here. Design modifications can be easily evaluated in a short time, therefore, reducing vehicle development time and cost.

REFERENCES

1 **Matteson, A.** and **Blower, D.** Trucks involved in fatal accidents. In *Codebook 2000*, 2003 (University of Michigan, Transportation Research Institute, Ann Arbor).
2 **North Carolina Department of Transportation Division of Motor Vehicles.** Driving combination vehicles safely (Internet) (cited 17th April), 2004, available from http://www.dmv.dot.state.nc.us/ driverlicense/ CDL/handbook/driving_combos.html.
3 **Gillespie, T. D.** *Fundamentals of vehicle dynamics*, 1992 (Society of Automotive Engineers, Warrendale, PA).
4 **Dixon, J. C.** *Tires, suspension and handling*, 1996 (Society of Automotive Engineers, Warrendale, PA; Arnold, London).
5 **Ellis, J. R.** *Vehicle handling dynamics*, 1994 (Mechanical Engineering Publications, Bury St Edmunds and London).
6 **Pacejka, H. B.** *Tyre and vehicle dynamics*, 2002 (Butterworth-Heinemann, Oxford).
7 **Rahnejat, H.** *Multibody dynamics: vehicles, machines, and mechanisms*, 1998 (Professional Engineering Publications, Bury St Edmunds and London, and Society of Automotive Engineers, Warrendale, PA (Co-publishers)).
8 **Hegazy, S., Rahnejat, H.,** and **Hussain, K.** Multibody dynamics in full-vehicle handling analysis. *Proc. Instn Mech. Engrs, Part K*: *J. Multi-body Dynamics*, 1999, **213**, 19–31.
9 **Hegazy, S., Rahnejat, H.,** and **Hussain, K.** Multibody dynamics in full-vehicle handling analysis under transient manoeuvre. *Vehicle Syst. Dyn.*, 2000, **34**, 1–24.
10 **Blundell, M.** and **Harty, D.** *Multibody systems approach to vehicle dynamics*, 2004 (Elsevier, Butterworth-Heinemann, Oxford).
11 **Genta, G.** *Motor vehicle dynamics: modeling and simulation*, 1997 (World Scientific Publishing, Singapore).
12 **Lin, R. C., Cebon, D.**, and **Cole, D. J.** An investigation of active roll control of heavy road vehicles. In Proceedings of 13th IAVSD Symposium, Chengdu, China, 1993.
13 **Sampson, D.** *Active roll control of articulated heavy vehicles*. PhD Thesis, Engineering Department, University of Cambridge, Cambridge.
14 **Aurell, J.** The influence of warp compliance on the handling and stability of heavy commercial vehicles. International Symposium on *Advanced vehicle control 2002*, Tokyo, 2002 (Society of Automotive Engineers of Japan, Japan).
15 *ADAMS (Automatic dynamic analysis of multibody systems) manual version 12, MSC.NASTRAN*, 2003.
16 **Pacejka, H. B.** and **Bakker, E.** The magic formula tyre model, tyre models for vehicle dynamic analysis. In Proceedings of the First International Colloquium on *Tyre models for vehicle dynamic analysis* (Ed. H. B. Pacejka) 1993, pp. 1–18 (Swets and Zeitlinger, Lisse).
17 **Da Cunha, R.** Handling analysis of a three-axle intercity bus. 16th European ADAMS User Conference 2001, Berchtesgaden, 2001 (MSC Software, Germany).
18 **Society of Automotive Engineers.** *Steady-state circular test procedure for trucks and buses*, 1998 (Society of Automotive Engineers, Warrendale, PA).
19 **Ross, C. F.** Electronic braking systems: an aid to vehicle stability. In *Braking of road vehicle*, 2004 (University of Bradford, UK) ISBN 1851432175.
20 **Gordon, T.** Multibody dynamic lecture notes, 2000. MSc course in Automotive Engineering (Department of Aeronautical and Automotive Engineering, University of Loughborough, UK).